DALTON
FULL PAPER

Bis(imino)pyridyl iron and cobalt complexes: the effect of nitrogen substituents on ethylene oligomerisation and polymerisation

George J. P. Britovsek,[a] Vernon C. Gibson,*[a] Brian S. Kimberley,[b] Sergio Mastroianni,[a] Carl Redshaw,[a] Gregory A. Solan,[a] Andrew J. P. White[a] and David J. Williams[a]

[a] *Department of Chemistry, Imperial College, London, UK SW7 2AY. E-mail: v.gibson@ic.ac.uk*
[b] *BP Chemicals Ltd., Sunbury Research Centre, Sunbury on Thames, Middlesex, UK TW16 7LN*

Received 6th February 2001, Accepted 15th March 2001
First published as an Advance Article on the web 25th April 2001

The synthesis and characterisation of 2,6-bis(imino)pyridyl iron and cobalt complexes [(2,6-(RN=CMe)$_2$C$_5$H$_3$N)-MCl$_2$] containing nitrogen substituents of the type R = NPh$_2$, NPhMe, NMe$_2$ or 2,5-dimethylpyrrolyl are described. These complexes, in combination with the co-catalyst MAO, give active catalysts for the oligomerisation or polymerisation of ethylene. The catalytic activity is strongly affected by the substituents R and the polymerisation conditions used. The polymer properties are also a function of the R substituents. With R = NPhMe or NMe$_2$, toluene soluble α-olefins are obtained, whereas the bulkier substituents (R = NPh$_2$ or 2,5-dimethylpyrrolyl) give low molecular weight solid polyethylene.

Introduction

The development of homogeneous organo-transition metal polymerisation catalysts has enabled the synthesis of polyolefinic materials with unprecedented levels of control over macromolecular structure. Although metallocene technology has been in the vanguard of these developments,[1–8] much recent work has focused on the search for non-metallocene catalysts, and indeed the armoury of available olefin polymerisation catalysts now traverses the entire transition metal series.[9]

One of the latest additions to the collection of highly active ethylene polymerisation catalysts is a family of iron and cobalt bis(imino)pyridyl catalysts of type **A** (Fig. 1), developed independently by Brookhart, Bennett and ourselves.[10,11] The versatility of these catalysts, in particular the ease of catalyst tuning by ligand variation, has already been amply demonstrated. For example, bulky aryl substituents provide catalysts for the polymerisation of ethylene that give high molecular weight, strictly linear polyethylene (HDPE)[12] whereas smaller substituents lead to the oligomerisation of ethylene to α-olefins.[13,14] As part of our ongoing investigations regarding the structure–activity relationships within this family of catalysts,[12,14,15] we report here new ethylene oligomerisation/polymerisation catalysts based on iron(II) and cobalt(II) complexes containing amine substituted bis(imino)pyridyl ligands of type **B** as shown in Fig. 1. Some of the results described here have been disclosed previously by us[16] and Eastman Chemical Company.[17]

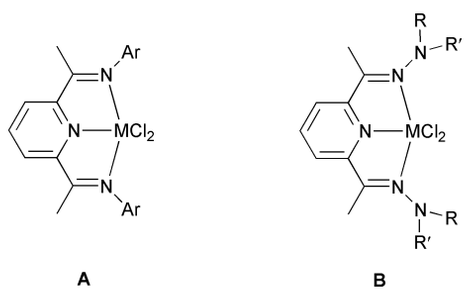

A **B**

Fig. 1 Bis(imino)pyridyl (**A**) and bis(hydrazone)pyridyl complexes (**B**).

Results and discussion

Synthesis of ligands and complexes

Bis(hydrazone)pyridine ligands **1a**–**c** were prepared from 2,6-diacetylpyridine and the appropriate hydrazine derivative, using a standard condensation protocol.[18] The synthesis of the pyrrolyl substituted ligand **1d** from 1-amino-2,5-dimethylpyrrole[19] required considerably longer reaction times to obtain satisfactory yields. Complexes **2a**–**d** and **3a**–**c** were readily prepared in good yields by reaction of $FeCl_2$ or $CoCl_2$ with the appropriate ligand according to Scheme 1.

The complexes are all highly coloured and paramagnetic with magnetic moments in the range of 5.1–5.3 μ_B (Evans balance) for the iron complexes and 4.6–4.8 μ_B for the cobalt complexes, consistent with four and three unpaired electrons respectively. ^{1}H NMR spectra show broad resonances in the range −60 to 80 ppm consistent with paramagnetic contact shifted resonances. The complexes have been further characterised by MS, microanalysis and X-ray analysis (see Experimental section).

Crystals of **2a**, **2c** and **3a** were grown by diffusion of pentane into the respective saturated dichloromethane solution at room temperature whilst crystals of **2b** were obtained from a saturated acetonitrile solution. The molecular structures of **2a**–**c** and **3a** have been determined. All four possess very similar gross overall structures, with those of the iron and cobalt complexes **2a** and **3a** being essentially isostructural (but not isomorphous). They all exhibit non-crystallographic C_s symmetry about a plane containing the metal atom, the pyridyl nitrogen and the two chloride ions (Figs. 2 and 3).

The geometries at the metal centres can be considered either as distorted square pyramidal with one of the chloride ions [Cl(1)] occupying the apical position, or as equally distorted trigonal bipyramidal with the pyridyl nitrogen atom, the metal centre and the two chlorides forming the equatorial plane. The ligand geometries (excluding the terminal amino substituents) are also, within statistical significance, the same. In all instances the imine C=N double bond character has been retained [C=N in the range 1.281(7)–1.293(6) Å] there being no evidence for

DOI: 10.1039/b101173l

Table 1 Selected bond lengths (Å) and angles (°) for **2a**, **2b**, **2c** and **3a**

	2a [M = Fe]	**2b** [M = Fe]	**2c** [M = Fe]	**3a** [M = Co]
M–Cl(1)	2.2872(14)	2.311(2)	2.299(2)	2.260(2)
M–Cl(2)	2.2565(13)	2.275(2)	2.294(2)	2.2480(14)
M–N(1)	2.085(4)	2.069(4)	2.079(4)	2.025(4)
M–N(8)	2.318(4)	2.279(4)	2.271(4)	2.250(4)
M–N(11)	2.283(4)	2.256(4)	2.285(4)	2.219(4)
Cl(1)–M–Cl(2)	136.45(6)	129.74(7)	129.95(6)	127.90(6)
Cl(1)–M–N(1)	95.68(11)	108.18(11)	111.37(12)	105.89(11)
Cl(1)–M–N(8)	99.48(10)	96.05(11)	96.75(11)	99.50(11)
Cl(1)–M–N(11)	95.06(10)	95.70(11)	97.52(12)	99.86(11)
Cl(2)–M–N(1)	127.86(11)	122.07(12)	118.69(11)	126.21(11)
Cl(2)–M–N(8)	94.58(10)	96.80(11)	96.93(12)	93.94(11)
Cl(2)–M–N(11)	96.00(10)	98.35(12)	95.80(11)	94.37(11)
N(1)–M–N(8)	73.65(14)	73.72(14)	73.8(2)	74.49(14)
N(1)–M–N(11)	74.05(14)	74.28(14)	74.1(2)	75.33(14)
N(8)–M–N(11)	145.63(14)	147.93(14)	147.7(2)	147.58(14)

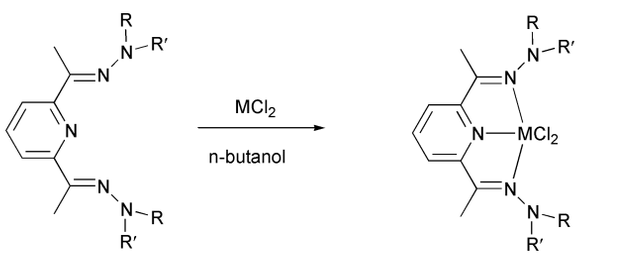

1a: R = R' = Ph
1b: R = Me, R' = Ph
1c: R = R' = Me

R = R' = Ph: M = Fe (**2a**), M = Co (**3a**)
R = Me, R' = Ph ; M = Fe (**2b**), M = Co (**3b**)
R = R' = Me ; M = Fe (**2c**), M = Co (**3c**)

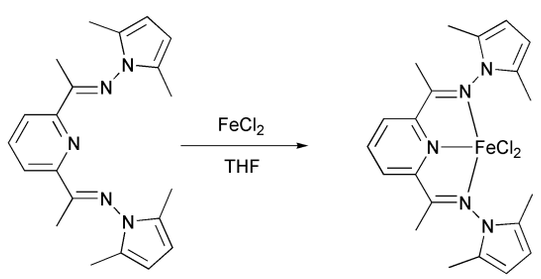

1d **2d**

Scheme 1

delocalisation into the adjacent hydrazido moieties which have distinctive single bond character [N–N 1.392(6)–1.423(6) Å]. The main differences between the four complexes are in the geometries and patterns of bonding around the metal centres and in the degree of pyramidalisation at the terminal hydrazido nitrogen centres (the latter being most pronounced in **2c**). Specifically, in the three iron complexes, the degree of pyramidalisation at the terminal nitrogen centres (defined by the displacement of the nitrogen out of the N–C–C plane) ranges from 0.19 Å in **2a** through 0.32 Å in **2b** to 0.48 Å in **2c**. In each case the nitrogen lone pair is directed away from the iron centre, thereby discounting any possible metal···lone pair interaction. Furthermore, there are in all three iron structures substantial torsional twists about the N–N bonds (ranging from 42° in **2b** to 57° in **2a**) thus precluding any significant N(pπ)–N(pπ) orbital overlap. As expected, the bonds to cobalt in **3a** are all shorter than their counterparts in the iron analogue **2a** (Table 1). In the three iron complexes the Fe–N(pyridyl) distances do not differ significantly. There are, however, some

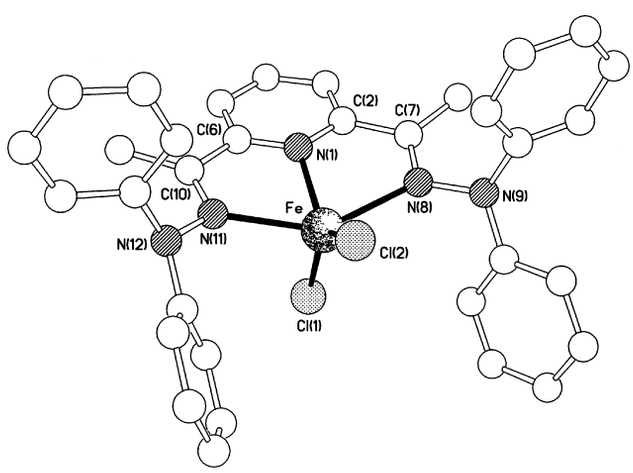

Fig. 2 The molecular structure of **2a** (that of **3a** is essentially isostructural).

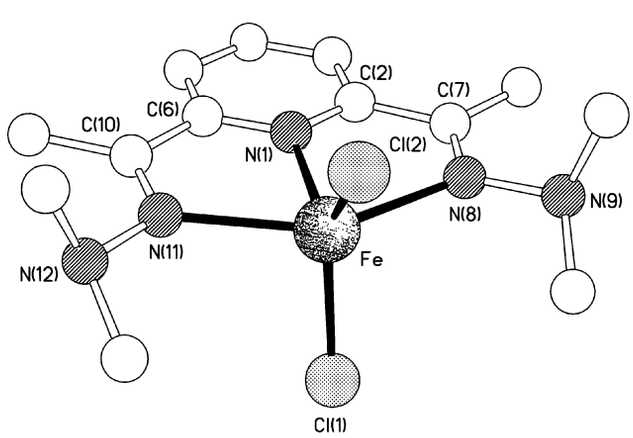

Fig. 3 The molecular structure of **2c**.

noticeable asymmetries in the Fe–N(imino) distances which are most pronounced in **2a** where the two distances are 2.283(4) and 2.318(4) Å, and least pronounced in the dimethylamino complex **2c** [2.271(4) and 2.285(4) Å]. These differences are probably related to the better σ-donating ability of dimethylamino *versus* diphenylamino substituents, resulting in increased electron density on the metal bound imine nitrogens. There are similar asymmetries in the Fe–Cl bond lengths which are most pronounced in **2b** and least in **2c**. These differences cannot be readily explained in terms of simple *trans* effects, due to the substantial departures from an idealised square pyramidal geometry.

The most dramatic differences are in the Cl(1)–M–Cl(2) and

Table 2 Results of ethylene polymerisation runs using complexes **2a**–**d**, **3a**–**c** and **4**

Run[a]	Pre-catalyst/ mmol	Co-catalyst (eq.)	Yield/g	Activity/g mmol^{-1} h^{-1} bar^{-1}	α[g]	M_w[h]	M_n[h]	M_w/M_n
1	**2a** (0.02)	MAO (200)	14.3[d]	71.5		2700	750	3.6
2[b]	**2a** (0.02)	MAO (100)	0.5/1.0[e]	473	0.84	900	700	1.3
3	**2b** (0.02)	MAO (200)	0.9[g]	4.4	0.51			
4	**2c** (0.02)	MAO (200)	0.5[g]	2.3	0.83			
5[b]	**2d** (0.01)	MAO (160)	0.4/0.8[e]	635	0.83	900	500	1.9
6[c]	**2d** (0.0005)	MAO (100)	15.7[f]	3140		900	500	1.9
7[i]	**4** (0.0006)	MAO (1000)	56.5	9340		242000	9600	25.3
8	**3a** (0.08)	MAO (200)	Trace	<1				
9	**3b** (0.08)	MAO (200)	1.9[g]	2.4	0.84			
10	**3c** (0.08)	MAO (200)	0.8[g]	1	0.75			

[a] Tests performed in 1 L autoclave, 10 bar ethylene pressure, 35 °C, isobutane solvent, pre-catalyst dissolved in toluene, MAO scavenger, 60 min. [b] Tests performed in a Schlenk flask, 0.75 bar ethylene pressure, 25 °C, toluene solvent (40 ml), 15 min. [c] Conditions as under *a*, except 50 °C and triisobutylaluminium as scavenger. [d] Solid polymer; saturated chain ends: 18.5 (/1000 C), vinyl chain ends: 17.2 (/1000 C), determined by ^{13}C NMR. [e] Solid polymer/oligomers in g. [f] Solid polymer; saturated chain ends: 22.1 (/1000 C), vinyl chain ends: 21.0 (/1000 C), determined by ^{13}C NMR. [g] Determined by GC. [h] Determined by GPC. [i] Results for pre-catalyst **4** taken from ref. 12.

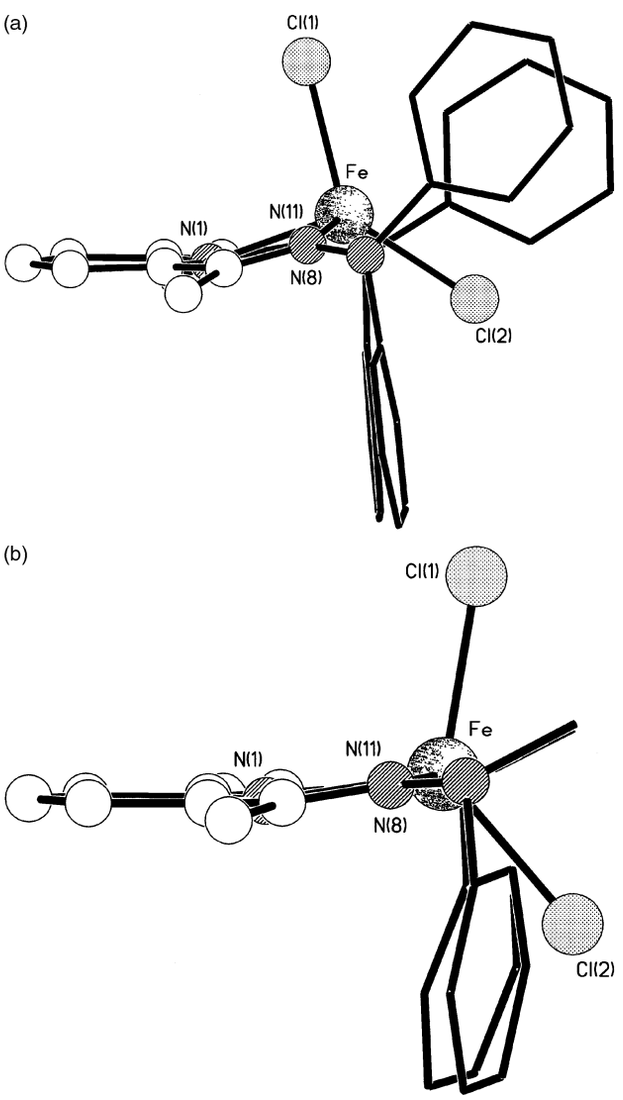

Fig. 4 Views down the N(8)···N(11) vector showing (a) the enlargement of the Cl(1)–Fe–Cl(2) angle and the tilting of the Fe–Cl(1) bond towards the pyridyl ring in **2a**, and (b) the contraction of the Cl(1)–M–Cl(2) angle and the tilting of the M–Cl(1) bond away from the pyridyl ring as seen in **2b**, **2c** and **3a** (that of **2b** is illustrated).

Cl(1)–M–N(1) angles in **2a**, which are substantially larger (by *ca.* 7°) and smaller (by *ca.* 13°) respectively, than in the others. This difference can be visualised in terms of the inclination of the "apical" M–Cl(1) vector to the basal plane, which in **2a** is 113.5° *cf.* values that range between 104.5 and 105.8° in the other complexes, this inclination being towards the pyridyl ring of the tridentate ligand (Fig. 4). There are no short intermolecular approaches to Cl(1) in any of the four structures.

Oligomerisation and polymerisation results

Bis(imino)pyridyl iron (**2a**–**d**) and cobalt (**3a**–**c**) complexes, in combination with the co-catalyst MAO, have been evaluated as catalysts for the polymerisation of ethylene. General reaction conditions are described in the Experimental section and the polymerisation results are summarised in Table 2.

Under Schlenk-line conditions (25 °C and 0.75 bar) and relatively short run times (15 minutes) complexes **2a** and **2d**, containing the diphenylamine and the 2,5-dimethylpyrrolyl substituents respectively, give a mixture of solid polyethylene and oligomers (ratio 1 : 2) with comparable activites (see Table 2, runs 2 and 5). Under high-pressure conditions (10 bar, 35 °C), the overall activity during one hour is considerably less for complexes **2a**–**c** than for the pyrrolyl substituted catalyst **2d**. The activity profiles[20] indicate that all catalysts **2a**–**d** give high initial activities but that the catalyst lifetime of **2d** is substantially longer than for **2a**–**c**, but not as long as for the previously reported catalyst **4**, containing 2,6-dimethylphenyl substituents (see Fig. 1, **A**, where Ar = 2,6-$Me_2C_6H_3$). For comparison, the polymerisation results of **4**, which were obtained under similar conditions, are also included in Table 2 (run 7).[12] Within the catalyst series **2a**–**c**, one possibility that could affect the catalyst stability and activity is the availability of the nitrogen lone pair of the NR_2 substituents for donation, either to the imine nitrogen or to the metal centre. In either case, this would reduce the electrophilicity of the metal centre, which would be expected to lower the activity. However, in the solid state structures of **2a**–**c**, the pyramidalisation of the amino nitrogen and the orientation of the NR_2 groups indicate that lone pair donation to the imine N {N(pπ)–N(pπ) overlap} is not strong (*vide supra*). The possibility of the amino group binding to the metal centre can be ruled out due to the constraints imposed by the ligand backbone. Another possibility is that, in the presence of MAO, it is very likely that $AlMe_3$ (or other aluminium centres in MAO) will bind to the nitrogen lone pair, in a similar manner to that observed for hydrazone derivatives of "constrained geometry" catalysts, which also gave much lower activities.[21,22] In the case of the 2,5-dimethylpyrrolyl catalyst derived from **2d**, the pyrrolyl nitrogen lone pair is not available for donation to the imine nitrogen due to the involvement in bonding within the pseudo-aromatic pyrrole ring and, for the same reason, it is also not available to donate to an external Lewis acid. Notwithstanding these arguments, it is also possible that the comparable activities of **2d** and **4** are mainly due to the steric resemblance of the

2,5-dimethylpyrrole and the 2,6-dimethylphenyl substituents. The cobalt precursors **3a**–**c** show generally lower activities compared to the iron analogues **2a**–**c**, in line with the differences in catalytic activity observed for iron *versus* cobalt bis(imino)-pyridine systems.[12]

All of the bis(imino)pyridyl iron and cobalt pre-catalysts tested in this study give relatively low molecular weight products. Within the iron series **2a**–**c**, at high pressure (10 bar), the diphenyl derivative **2a** gives solid polymer with a relatively low molecular weight ($M_w = 2700$), whereas the Me/Ph and dimethyl derivatives **2b** and **2c** give toluene soluble oligomers. At lower temperature and pressure, **2a** gives a mixture of oligomers and polymer (run 2). The oligomeric products have been shown by GC/MS to consist of linear α-olefins following a typical Schulz–Flory distribution. The distribution factors α are listed in Table 2. The reason for the lower α-value of **2b** compared to **2a** is unclear at present, but these values are subject to a relatively large error due to the very low activity of these catalysts. In the case of bis(imino)pyridyl iron and cobalt catalysts, the molecular weight of the polymer product is strongly affected by the size of the aryl substituents. With this in mind, it is rather surprising to see that the 2,5-dimethylpyrrolyl derivative **2d** produces low molecular weight polyethylene ($M_w = 900$), whereas the 2,6-dimethylphenyl analogue **4**, which is believed to possess comparable steric requirements, gives high molecular weight polymer ($M_w = 242000$). This result indicates that the size and shape of the substituent on the imino nitrogen, allowing for the differences between six- and five-membered rings, are not the only factors responsible for the formation of high molecular weight polymers and that electronic effects may be more important than realised to date.

End-group analysis of the polymers produced by **2a** and **2d** by ^{1}H and ^{13}C NMR has shown an equal amount of saturated and vinyl terminated ends (see Table 2). This analysis shows that these low molecular weight polymers are α-olefins, generated by a termination pathway *via* β-H transfer, similar to the oligomerisation catalysts **2b** and **2c**. No chain transfer to aluminium is observed under these conditions, a transfer process that only seems to become competitive with β-H transfer when higher molecular weight polyethylene is produced, *i.e.* when the rate of β-H transfer is sufficiently low.

In conclusion, we have shown that bis(imino)pyridyl iron and cobalt dichloride complexes containing nitrogen substituents can be readily synthesised and provide active catalysts for the polymerisation of ethylene after activation with MAO. As seen before, iron derived catalysts are, in general, much more active than their cobalt analogues. Within the iron series tested here, the catalytic activity obtained with pre-catalyst **2d** containing 2,5-dimethylpyrrolyl substituents, is, under certain conditions significantly higher than for **2a**–**c**. The activity profile indicates that the lifetime of the catalyst derived from **2d** is longer than for **2a**–**c** but not as long as for the aryl substituted derivatives such as **4**. All iron and cobalt catalysts tested here give relatively low molecular weight polyethylene or oligomers, with vinyl end-groups in all cases.

Experimental

General

All manipulations were carried out under an atmosphere of nitrogen using standard Schlenk and cannula techniques or in a conventional nitrogen-filled glove-box. Solvents were refluxed over an appropriate drying agent, and distilled and degassed prior to use. Elemental analyses were performed by the microanalytical services of the Department of Chemistry at Imperial College, Medac Ltd. or SACS at the University of North London. NMR spectra were recorded on a Bruker spectrometer at 250 MHz (^{1}H), and 62.9 MHz (^{13}C) at 293 K; chemical shifts are referenced to the residual protio impurity of the deuterated solvent. Mass spectra were obtained using either Fast Atom Bombardment (FAB), Electron Impact (EI) or Chemical Ionization (CI). IR spectra were recorded on a Perkin-Elmer Spectrum GX1 System. Samples were prepared by evaporating CH_2Cl_2 solutions of the ligands or complexes on NaCl plates. Magnetic susceptibility studies were performed using an Evans' balance.

Materials

1-Amino-2,5-dimethylpyrrole was prepared according to a procedure by Zimmermann,[19] while 2,6-diacetylpyridine, MAO (10% solution in toluene) and all hydrazines were purchased from Aldrich Chemical Co. All other chemicals were obtained commercially and used as received unless stated otherwise.

Preparations

2,6-Diacetylpyridinebis(*N*,*N*-diphenylhydrazone) (1a). 1,1-Diphenylhydrazine hydrochloride (6 g, 0.027 mol) in dichloromethane (50 ml) was treated with gaseous ammonia for 30 min at room temperature. After filtration, the solvent was removed under vacuum to afford *N*,*N*-diphenylhydrazine as a viscous oil (yield 4.7 g, 95%). To a solution of 2,6-diacetylpyridine (1.67 g, 0.01 mol) in absolute ethanol (30 ml) was added *N*,*N*-diphenylhydrazine (4.7 g, 0.025 mol). After addition of a few drops of glacial acetic acid the solution was refluxed for 4 hours. Volatiles were removed under vacuum and the solid was washed with cold ethanol and dried in a vacuum oven (50 °C) overnight to give 5.9 g (92%) of **1a**. ^{1}H NMR data (250 MHz, $CDCl_3$, 298 K): δ 8.32 (d, 2H, ^3J(HH) 7.9, Py-H_m), 7.75 (t, 1H, Py-H_p), 7.35–7.06 (m, 20H, Ar-*H*), 2.21 (s, 6H, N=CCH_3). MS (EI, *m*/*z*) 495 $[M]^+$. ^{13}C NMR (100 MHz, $CDCl_3$, 298 K): δ 161.9 (N=*C*), 155.0 (Ar-*C*), 148.2 (Py-C_o), 136.3 (Py-C_p), 129.1 (Ar-*C*), 123.5 (Ar-*C*), 121.8 (Py-C_m), 121.0 (Ar-*C*), 17.8 (N=C*C*H$_3$). IR (CH_2Cl_2 film, NaCl, cm^{-1}) 3059 (br), 1588 (s), 1561 (m), 1488 (vs), 1451 (s), 1364 (w), 1270 (m), 1201 (s), 1179 (w), 1086 (w), 1049 (w), 843 (w), 819 (w), 750 (s), 629 (s). Elemental analysis for $C_{33}H_{29}N_5$ (495.63) found (required): %C = 79.5 (80.0), %H = 5.8 (5.9), %N = 13.9 (14.1).

2,6-Diacetylpyridinebis(*N*-methyl-*N*-phenylhydrazone) (1b). Procedure as described for **1a**, using 2,6-diacetylpyridine (1.67 g, 0.01 mol) and *N*-methyl-*N*-phenylhydrazine (3.05 g, 0.025 mmol). **1b** was obtained in 83% yield (3.08 g). ^{1}H NMR (250 MHz, $CDCl_3$, 298 K): δ 8.27 (d, 2H, ^3J(HH) 7.9 Hz, Py-H_m), 7.75 (t, 1H, Py-H_p), 7.35–7.05 (m, 10 H, Ar-*H*), 3.28 (s, 6H, N-CH_3), 2.21 (s, 6H, N=CCH_3). ^{13}C NMR (100 MHz, $CDCl_3$, 298 K): δ 163.8 (N=*C*), 154.9 (Ar-*C*), 151.1 (Py-C_o), 136.3 (Py-C_p), 128.9 (Ar-*C*), 121.1 (Ar-*C*), 120.4 (Py-C_m), 115.7 (Ar-*C*), 42.9 (N–*C*H$_3$) 15.8 (N=C*C*H$_3$). MS (EI, *m*/*z*) 371 $[M]^+$. IR: (CH_2Cl_2 film, NaCl, cm^{-1}) 3067 (m), 2875 (br), 2798 (w), 1599 (vs), 1567 (vs), 1494 (vs), 1453 (vs), 1362 (s), 1286 (m), 1250 (m), 1185 (m), 1091 (vs), 996 (m), 879 (w), 837 (m), 819 (s), 788 (m), 753 (vs), 692 (vs), 647 (w), 520 (m). Elemental analysis for $C_{23}H_{25}N_5$ (371.48) found (required): %C = 74.9 (74.4), %H = 6.4 (6.8), %N = 18.0 (18.8).

2,6-Diacetylpyridinebis(*N*,*N*-dimethylhydrazone) (1c). Procedure as described for **1a**, using 2,6-diacetylpyridine (1.63 g, 0.01 mol) and *N*,*N*-dimethylhydrazine (1.6 ml, 0.021 mmol), **1c** was obtained as a viscous oil in 78% yield (1.93 g). ^{1}H NMR (250 MHz, C_6D_6, 298 K): δ 8.19 (d, 2H, ^3J(HH) 7.9 Hz, Py-H_m), 7.15 (t, 1H, Py-H_p), 2.53 (s, 12H, N(CH_3)$_2$), 2.50 (s, 6H, N=CCH_3). ^{13}C NMR (100 MHz, C_6D_6, 298 K): δ 161.3 (N=*C*), 155.5 (Py-C_o), 135.8 (Py-C_p), 120.5 (Py-C_m), 47.2 [N(*C*H$_3$)$_2$], 14.3 (N=C*C*H$_3$). IR (CH_2Cl_2 film, NaCl, cm^{-1}): 2991 (s), 2956 (vs), 2858 (vs), 2820 (vs), 2776 (s), 1608 (w), 1569 (s), 1454 (vs), 1361 (s), 1256 (m), 1208 (w), 1148 (m), 1120 (s), 1100 (m), 1079 (m), 1014 (vs), 991 (m), 960 (m), 876 (m), 814 (vs), 742 (m), 639

(m). Elemental analysis for $C_{13}H_{21}N_5$ (247.34) found (required): %C = 62.9 (63.1), %H = 8.4 (8.6), %N = 27.7 (28.3).

2,6-Diacetylpyridinebis(2,5-dimethylpyrrolyl) (1d). A solution of 1-amino-2,5-dimethylpyrrole (0.66 g, 6 mmol) and 2,6-diacetylpyridine (0.49 g, 3 mmol) in 20 ml toluene was refluxed for 5 days in the presence of molecular sieves (4 Å) and a drop of glacial acetic acid. After filtration the solvent was removed and the oily residue recrystallised from ethanol, yielding **1d** as a yellow solid (0.85 g, 82%). ^{1}H NMR (250 MHz, $CDCl_3$, 298 K): δ 8.47 (d, 2H, ^3J(HH) 7.9 Hz, Py-H_m), 7.94 (t, 1H, Py-H_p), 5.91 (s, 4H, pyrrole *CH*), 2.37 (s, 6H, N=CCH_3), 2.09 (s, 12H, pyrrole CH_3). ^{13}C NMR (100 MHz, $CDCl_3$, 298 K): δ 176.1 (N=*C*), 153.5 (Py-C_o), 137.2 (Py-C_p), 123.7 (Py-C_m), 123.5 (pyrrole *C*CH_3), 103.8 (pyrrole *C*H), 15.51 (N=*C*CH_3), 11.82 (pyrrole *C*H_3). MS (EI, *m*/*z*): 347 $[M]^+$, 253 $[M - C_6H_8N]^+$. IR (neat, NaCl, cm^{-1}): 3100 (w), 2976 (m), 2921 (s), 2891 (m), 2857 (w), 2235 (w), 1702 (w), 1613 (s), 1570 (s), 1514 (w), 1440 (s), 1391 (vs), 1370 (vs), 1290 (s), 1128 (m), 1020 (m), 911 (s), 822 (s), 737 (vs). Elemental analysis for $C_{21}H_{25}N_5$ (347.47) found (required): %C = 72.6 (72.6), %H = 7.4 (7.3), %N = 20.1 (20.2).

2,6-Diacetylpyridinebis(*N*,*N*-diphenylhydrazone)iron dichloride (2a). A suspension of $FeCl_2$ (0.184 g, 1.41 mmol) and **1a** (0.70 g, 1.41 mmol) was prepared in n-butanol (20 ml) which was then heated at 90 °C for 30 min. The resultant dark product, which precipitated from solution, was filtered off and washed several times with diethyl ether (3 × 20 ml) and dried to afford 0.79 g (89%) of **2a**. The complex could additionally be recrystallised by slow diffusion of pentane into a saturated solution of **2a** in dichloromethane to give brown needles. ^{1}H NMR data (250 MHz, CD_2Cl_2, 298 K, broad singlets are observed in each case): δ 72.1 (2H, Py-H_m), 20.0 (6H, N=CCH_3), 2.1 (8H, Ar-*H*), 1.6 (8H, Ar-*H*), 1.3 (4H, Ar-H_p), −8.7 (1H, Py-H_p). MS (FAB, *m*/*z*) 621 $[M]^+$, 586 $[M - Cl]^+$. IR: (CH_2Cl_2 film, NaCl, cm^{-1}) 3059 (w), 1588 (vs), 1521 (w), 1491 (w), 1450 (w), 1369 (w), 1291 (m), 1269 (w), 1213 (m), 1083 (w), 1061 (w), 1023 (w), 752 (vs), 693 (vs). Elemental analysis for $C_{33}H_{29}N_5FeCl_2 \cdot 0.75CH_2Cl_2$ (686.08) found (required): %C = 59.1 (59.5), %H = 4.4 (4.5), %N = 10.1 (10.2). μ_{eff} (Evans Balance): 5.15 μ_B.

2,6-Diacetylpyridinebis(*N*-methyl-*N*-phenylhydrazone)iron dichloride (2b). The procedure as above for complex **2a**, using **1b** (0.464 g, 1.25 mmol) and $FeCl_2$ (152 mg, 1.2 mmol) gave **2b** as a brown powder in 88% yield (0.54 g). The complex could additionally be recrystallised from boiling acetonitrile to give brown needles. ^{1}H NMR (250 MHz, CD_2Cl_2, 298 K, broad singlets are observed in each case): δ 69.5 (2H, Py-H_m), 28.6 (6H, N=CCH_3), 16.1 (6H, N(CH_3)$_2$), 13.4 (4H, Ar-*H*), 10.1 (Ar-*H*), 8.5 (Ar-H_p), −30.0 (1H, Py-H_p). MS (FAB, *m*/*z*): 497 $[M]^+$, 462 $[M - Cl]^+$. IR: (CH_2Cl_2 film, NaCl, cm^{-1}): 3047 (m), 2974 (m), 2893 (w), 2808 (w), 1594 (vs), 1538 (s), 1455 (s), 1371 (m), 1263 (vs), 1197 (s), 1100 (s), 1028 (s), 964 (m), 940 (w), 837 (w), 809 (m), 764 (s), 737 (vs), 698 (vs), 677 (w), 564 (w), 523 (m). Elemental analysis for $C_{23}H_{25}N_5FeCl_2$ (498.24) found (required): %C = 55.2 (55.5), %H = 5.3 (5.1), %N = 13.9 (14.1). μ_{eff} (Evans Balance): 5.28 μ_B.

2,6-Diacetylpyridinebis(*N*,*N*-dimethylhydrazone)iron dichloride (2c). The procedure as for complex **2a**, using **1c** (0.370 g, 1.5 mmol) and $FeCl_2$ (0.190 g, 1.5 mmol) gave **2c** as a brown powder in 88% yield (0.49 g). The complex could be recrystallised by slow diffusion of pentane into a saturated solution of **2c** in dichloromethane to give brown needles. ^{1}H NMR (250 MHz, CD_2Cl_2, 298 K, broad singlets are observed in each case): δ 69.4 (2H, Py-H_m), 25.3 (6H, N=CCH_3), 20.0 (12H, N(CH_3)$_2$), −24.5 (1H, Py-H_p). MS (FAB, *m*/*z*): 373 $[M]^+$, 338 $[M - Cl]^+$. IR (CH_2Cl_2 film, NaCl, cm^{-1}): 3064 (w), 3000 (w), 2957 (m), 2879 (s), 28230 (w), 2794 (m), 1599 (m), 1571 (m), 1546 (m), 1468 (m) 1450 (s), 1401 (w), 1361 (s), 1269 (m), 1191 (m), 1030 (vs), 1010 (m), 957 (m), 813 (vs), 745 (m), 557 (w). Elemental analysis for $C_{13}H_{21}N_5FeCl_2$ (374.20) found (required): %C = 41.4 (41.7), %H = 5.1 (5.6), %N = 18.3 (18.7). μ_{eff} (Evans Balance) 5.27 μ_B.

2,6-Diacetylpyridinebis(2,5-dimethylpyrrolyl)iron dichloride (2d). A solution of **1d** (190 mg; 0.55 mmol) in 10 ml THF was added to a suspension of $FeCl_2$ in THF. The mixture was stirred for 3 hours at room temperature. The volume of the dark solution was reduced to 5 ml and the product precipitated with diethyl ether. The product **2d** was washed with diethyl ether and dried *in vacuo*, yielding a dark green powder in 85% yield (222 mg). ^{1}H NMR (250 MHz, CD_2Cl_2, 298 K, broad singlets are observed in each case): δ 66.9 (2H, Py-H_m), 48.3 (1H, Py-H_p), 3.6–1.8 (16H, pyrrole CH_3 and C*H*), −40.1 (6H, N=CCH_3). MS (FAB, *m*/*z*): 474 $[M]^+$, 438 $[M - Cl]^+$. IR (neat, cm^{-1}): 3369 (br, m), 2919 (m), 1580 (m), 1440 (w), 1387 (vs), 1267 (m), 1206 (m), 1019 (m), 811 (w), 737 (vs). Elemental analysis for $C_{21}H_{25}N_5FeCl_2$ (474.22) found (required): %C = 53.0 (53.2), %H = 5.4 (5.3), %N = 14.7 (14.8).

2,6-Diacetylpyridinebis(*N*,*N*-diphenylhydrazone)cobalt dichloride (3a). The procedure as for complex **2a**, using **1a** (0.619 g, 1.25 mmol) and $CoCl_2$ (0.162 g, 1.25 mmol) gave **3a** as a brown powder in 91% yield (0.71 g). The complex could additionally be recrystallised by slow diffusion of pentane into a saturated solution of **3a** in dichloromethane to give brown needles. ^{1}H NMR (250 MHz, CD_2Cl_2, 298 K, broad singlets are observed in each case): δ 75.5 (2H, Py-H_m), 0.1 (4H, Ar-H_p), −0.7 (8H, Ar-*H*), −1.1 (1H, Py-H_p) −10.4 (6H, N=CCH_3), −24.5 (8H, Ar-*H*). IR (neat, cm^{-1}): 3060 (w), 2963 (w), 1578 (s), 1521 (w), 1491 (vs), 1372 (w), 1269 (m), 1213 (m), 1064 (m), 1027 (w), 804 (w), 752 (m), 693 (m). MS (FAB, *m*/*z*) 589 $[M - Cl]^+$. Elemental analysis for $C_{33}H_{29}N_5CoCl_2 \cdot CH_2Cl_2 \cdot H_2O$ (728.42) found (required): %C = 56.1 (56.1), %H = 4.1 (4.6), %N = 9.5 (9.6). μ_{eff} (Evans Balance): 4.65 μ_B.

2,6-Diacetylpyridinebis(*N*-methyl-*N*-phenylhydrazone)cobalt dichloride (3b). The procedure as for complex **2a**, using **1b** (0.464 g, 1.25 mmol) and $CoCl_2$ (162 mg, 1.25 mmol) gave **3b** as a brown powder in 92% yield (0.58 g). The complex could be recrystallised by slow diffusion of pentane into a saturated solution of **3b** in dichloromethane to give brown needles. ^{1}H NMR (250 MHz, CD_2Cl_2, 298 K, broad singlets are observed in each case): δ 79.5 (2H, Py-H_m), 2.9 (4H, Ar-*H*), 1.7 (2H, Ar-H_p), −12.5 (4H, Ar-*H*), −14.1 (1H, Py-H_p), −19.1 (6H, N=CCH_3), −51.8 (6H, NCH_3). MS (FAB, *m*/*z*): 500 $[M]^+$, 465 $[M - Cl]^+$. IR (neat, cm^{-1}): 3044 (w), 2970 (w), 2895 (w), 1591 (s), 1528 (m), 1491 (vs), 1450 (m), 1368 (w), 1264 (m), 1097 (m), 1027 (m), 960 (w), 808 (w), 760 (m), 737 (m), 697 (m). Elemental analysis for $C_{23}H_{25}N_5CoCl_2 \cdot 1/3CH_2Cl_2$ (529.65) found (required): %C = 53.0 (52.9), %H = 5.0 (4.9), %N = 13.1 (13.2). μ_{eff} (Evans Balance): 4.72 μ_B.

2,6-Diacetylpyridinebis(*N*,*N*-dimethylhydrazone)cobalt dichloride (3c). The procedure as for complex **2a**, using **1c** (0.370 g, 1.5 mmol) and $CoCl_2$ (0.193 g, 1.5 mmol) gave **3c** as a brown powder in 62% yield (0.35 g). The complex could additionally be recrystallised by slow diffusion of pentane into a saturated solution of **3c** in dichloromethane to give brown needles. ^{1}H NMR (250 MHz, CD_2Cl_2, 298 K, broad singlets are observed in each case): δ 77.4 (2H, Py-H_m), −12.5 (1H, Py-H_p), −18.0 (6H, N=CCH_3), −36.3 [12H, N(CH_3)$_2$]. MS (FAB, *m*/*z*): 373 $[M]^+$, 338 $[M - Cl]^+$. IR (neat, cm^{-1}): 3052 (w), 2925 (w), 2851 (w0, 1599 (w), 1543 (w), 1447 (br), 1361 (w), 1264 (vs), 1186 (w), 1027 (w), 808 (w), 741 (vs), 704 (m). Elemental analysis for $C_{13}H_{21}N_5CoCl_2 \cdot 1/3H_2O$ (383.18) found (required): %C = 40.8 (40.8), %H = 5.3 (5.7), %N = 17.9 (18.3). μ_{eff} (Evans Balance): 4.69 μ_B.

Crystallography

2a: $C_{33}H_{29}N_5Cl_2Fe\cdot0.5CH_2Cl_2$, $M = 664.8$, orthorhombic, *Pbca* (no. 61), $a = 15.877(2)$, $b = 17.546(3)$, $c = 22.725(4)$ Å, $V = 6331(2)$ Å^3, $Z = 8$, $D_c = 1.395$ g cm^{-3}, μ(Cu-Kα) = 64.0 cm^{-1}, $T = 293$ K, dark red platy needles; 4609 independent measured reflections, F^2 refinement, $R_1 = 0.050$, $wR_2 = 0.113$, 3062 independent observed absorption corrected reflections [$|F_o| > 4\sigma(|F_o|)$, $2\theta \leq 120°$], 352 parameters.

2b: $C_{23}H_{25}N_5Cl_2Fe\cdot MeCN$, $M = 539.3$, monoclinic, $P2_1/c$ (no. 14), $a = 13.729(1)$, $b = 13.277(1)$, $c = 15.059(2)$ Å, $\beta = 101.81(1)°$, $V = 2686.7(5)$ Å^3, $Z = 4$, $D_c = 1.333$ g cm^{-3}, μ(Cu-Kα) = 65.2 cm^{-1}, $T = 293$ K, deep red platy needles; 3690 independent measured reflections, F^2 refinement, $R_1 = 0.053$, $wR_2 = 0.128$, 2692 independent observed absorption corrected reflections [$|F_o| > 4\sigma(|F_o|)$, $2\theta \leq 120°$], 284 parameters.

2c: $C_{13}H_{21}N_5Cl_2Fe$, $M = 374.1$, monoclinic, $P2_1/n$ (no. 14), $a = 8.909(1)$, $b = 17.133(1)$, $c = 11.054(1)$ Å, $\beta = 94.07(1)°$, $V = 1683.0(2)$ Å^3, $Z = 4$, $D_c = 1.476$ g cm^{-3}, μ(Cu-Kα) = 101.1 cm^{-1}, $T = 293$ K, dark brown prisms; 2491 independent measured reflections, F^2 refinement, $R_1 = 0.051$, $wR_2 = 0.118$, 1883 independent observed absorption corrected reflections [$|F_o| > 4\sigma(|F_o|)$, $2\theta \leq 120°$], 191 parameters.

3a: $C_{33}H_{29}N_5Cl_2Co\cdot1.5CH_2Cl_2$, $M = 752.8$, tetragonal, $I4_1/a$ (no. 88), $a = 20.698(2)$, $c = 33.803(3)$ Å, $V = 14482(2)$ Å^3, $Z = 16$, $D_c = 1.381$ g cm^{-3}, μ(Mo-Kα) = 8.74 cm^{-1}, $T = 293$ K, deep red needles; 6333 independent measured reflections, F^2 refinement, $R_1 = 0.058$, $wR_2 = 0.118$, 3823 independent observed reflections [$|F_o| > 4\sigma(|F_o|)$, $2\theta \leq 50°$], 390 parameters.

CCDC reference numbers 158046–158049.

See http://www.rsc.org/suppdata/dt/b1/b101173l/ for crystallographic data in CIF or other electronic format.

General polymerisation procedures

(a) High-pressure tests. A 1 litre stainless steel reactor was baked out under a nitrogen flow for at least 1 hour at >85 °C and subsequently cooled to the temperature of polymerization. Isobutane (0.5 L) and trialkylaluminium (triisobutylaluminium) were introduced into the reactor and stirred at reaction temperature for at least 1 hour. Ethylene was introduced by over-pressure and the difference between the total pressure and the initial pressure (isobutane and nitrogen: *ca.* 10 bar) is the pressure quoted in Table 2. The catalyst solution in toluene was then injected under nitrogen. The reactor pressure was maintained constant throughout the polymerisation run by computer controlled addition of ethylene. The polymerisation time was 60 min. Runs were terminated by venting off volatiles and the reactor contents were isolated, washed with aqueous HCl, methanol and dried in a vacuum oven at 50 °C.

(b) Schlenk-flask ethylene polymerisation tests. The pre-catalyst was dissolved in toluene (40 ml) and MAO (10 wt% in toluene) added to produce an orange solution. The Schlenk tube was placed in a water bath, purged with ethylene and the contents magnetically stirred and maintained under ethylene (0.75 bar over-pressure) for the duration of the polymerisation (15 min). The polymerisation was terminated by the addition of aqueous hydrogen chloride. The solid PE was recovered by filtration, washed with methanol (50 mL) and dried (vacuum oven at 50 °C).

Acknowledgements

BP Chemicals Ltd. are thanked for financial support. Drs J. Boyle, C. Baker and G. Audley are thanked for NMR and GPC measurements and Mr J. Barton for GC analyses. Dr P. Maddox is thanked for helpful discussions.

References

1 H. H. Brintzinger, D. Fischer, R. Mülhaupt, B. Rieger and R. M. Waymouth, *Angew. Chem.*, *Int. Ed. Engl.*, 1995, **34**, 1143.
2 M. Bochmann, *J. Chem. Soc.*, *Dalton Trans.*, 1996, 255.
3 W. Kaminsky, *J. Chem. Soc.*, *Dalton Trans.*, 1998, 1413.
4 P. C. Möhring and N. J. Coville, *J. Organomet. Chem.*, 1994, **479**, 1.
5 E. Albizzati and M. Galimberti, *Catal. Today*, 1998, **41**, 159.
6 A. M. Thayer, *Chem. Eng. News*, 1995, Sept 11, 15.
7 K. B. Sinclair and R. B. Wilson, *Chem. Ind.*, 1994, 857.
8 A. A. Montagna, R. M. Burkhart and A. H. Dekmezian, *CHEMTECH*, 1997, December, 26.
9 G. J. P. Britovsek, V. C. Gibson, D. F. Wass, *Angew. Chem.*, *Int. Ed.*, 1999, **38**, 428.
10 B. L. Small, M. Brookhart and A. M. A. Bennett, *J. Am. Chem. Soc.*, 1998, **120**, 4049.
11 G. J. P. Britovsek, V. C. Gibson, B. S. Kimberley, P. J. Maddox, S. J. McTavish, G. A. Solan, A. J. P. White and D. J. Williams, *Chem. Commun.*, 1998, 849.
12 G. J. P. Britovsek, M. Bruce, V. C. Gibson, B. S. Kimberley, P. J. Maddox, S. Mastroianni, S. J. McTavish, C. Redshaw, G. A. Solan, S. Strömberg, A. J. P. White and D. J. Williams, *J. Am. Chem. Soc.*, 1999, **121**, 8728.
13 B. L. Small and M. Brookhart, *J. Am. Chem. Soc.*, 1998, **120**, 7143.
14 G. J. P. Britovsek, S. Mastroianni, G. A. Solan, S. P. D. Baugh, C. Redshaw, V. C. Gibson, A. J. P. White, D. Williams and M. R. J. Elsegood, *Chem. Eur. J.*, 2000, **6**, 2221.
15 G. J. P. Britovsek, V. C. Gibson, S. Mastroianni, D. C. H. Oakes, C. Redshaw, G. A. Solan, A. J. P. White and D. Williams, *Eur. J. Inorg. Chem.*, 2001, 431.
16 G. J. P. Britovsek, B. A. Dorer, V. C. Gibson, B. S. Kimberley and G. A. Solan, BP Chemicals Ltd., *World Pat.*, WO 99/12981, 1999; G. J. P. Britovsek, B. A. Dorer, V. C. Gibson, B. S. Kimberley and G. A. Solan, *Chem. Abstr.*, 1999, **130**, 252793.
17 L. S. Moody, P. B. Mackenzie, C. M. Killian, G. G. Lavoie, J. A. Ponasik Jr., A. G. M. Barrett, T. W. Smith and J. C. Pearson, Eastman Chemical Company, *World Pat.*, WO 00/50470, 2000; L. S. Moody, P. B. Mackenzie, C. M. Killian, G. G. Lavoie, J. A. Ponasik Jr., A. G. M. Barrett, T. W. Smith and J. C. Pearson, *Chem. Abstr.*, 2000, **133**, 208316.
18 J. D. Curry, M. A. Robinson and D. H. Busch, *Inorg. Chem.*, 1967, **6**, 1570.
19 W. Flitsch, U. Krämer and H. Zimmermann, *Chem. Ber.*, 1969, **102**, 3268.
20 Catalyst activities, which are commonly expressed in g mmol^{-1} h^{-1} bar^{-1} give an average value for the activity during one hour. It should be noted however, that catalyst activities are rarely constant over an extended period of time and, for a meaningful comparison of catalyst activities, the kinetic profile (ethylene uptake over time) needs to be taken into account.
21 S. C. Yoon, B.-J. Bae, I.-H. Suh and J. T. Park, *Organometallics*, 1999, **18**, 2049.
22 J. T. Park, S. C. Yoon, B.-J. Bae, W. S. Seo, I.-H. Suh, T. K. Han and J. R. Park, *Organometallics*, 2000, **19**, 1269.